PHYSICAL REVIEW E **74**, 040501(R) (2006)

Universality in the phase behavior of soft matter: A law of corresponding states

G. Malescio
Dipartimento di Fisica, Università di Messina, 98166 Messina, Italy

(Received 14 June 2006; revised manuscript received 4 August 2006; published 26 October 2006)

We show that the phase diagram of substances whose molecular structure changes upon varying the thermodynamic parameters can be mapped, through state-dependent scaling, onto the phase diagram of systems of molecules having fixed structure. This makes it possible to identify broad universality classes in the complex phase scenario exhibited by soft matter, and enlightens a surprisingly close connection between puzzling phase phenomena and familiar behaviors. The analysis presented provides a straightforward way for deriving the phase diagram of soft substances from that of simpler reference systems. This method is applied here to study the phase behavior exhibited by two significative examples of soft matter with temperature-dependent molecular structure: thermally responsive colloids and polymeric systems. A region of inverse melting, i.e., melting upon isobaric cooling, is predicted at relatively low pressure and temperature in polymeric systems.

DOI: 10.1103/PhysRevE.74.040501 PACS number(s): 64.70.−p, 64.60.−i, 05.70.Fh

Soft matter [1,2] encompasses an ample class of substances of growing biological and industrial relevance, such as colloidal systems, polymers, and surfactants, characterized by supramolecular architecture largely susceptible to external agents. One of their most important features is the peculiar phase behavior [3], which is relevant for fundamental reasons and technological applications. Due to the growing ability to tune interactions at microscopic level [4], recent years have witnessed a burgeoning increment of exotic phase phenomena, which makes soft matter phase behavior panorama more and more rich and challenging to interpret. This situation calls for a unifying approach offering a wide-angle perspective able to enlighten cross-relations between apparently unrelated phase phenomena.

Scaling represents a simple and effective tool for the individuation of universal behaviors. It has often been used in investigating phase transitions, starting from Van der Waals' law of corresponding states (LCS) [5–7], arguably its first application. The essential point of LCS is that a *single* reference system can account, upon appropriate rescaling, for the properties of atomic fluids. A similar idea, suitably generalized, informs our investigation. We show that the phase behavior of soft substances, i.e., substances whose structure changes upon varying thermodynamic parameters, can be accounted for by a *family* of reference systems with state-independent structure. We represent intermolecular interactions within an effective potential approach and assume that the total intermolecular potential U can be expressed as a sum over pair potentials written as an energy parameter ε times a function of the reduced intermolecular distance r/σ, i.e., $U=\Sigma_{ij}u(r_{ij})$, $u(r_{ij})=\varepsilon f(r_{ij}/\sigma)$. The effect of variations of the molecular structure on the interaction potential is taken into account through state-dependent energy and size parameters, that represent in an average way the presence of internal degrees of freedom. This can be considered as a first-order approximation, in which modifications of the molecular structure are assumed to affect ε and σ, while the functional form of the pair potential remains unaltered. The intermolecular potential can then be explicitly written as $u_{VAR}(r,X)=\varepsilon(X)f[r/\sigma(X)]$, where X is the vector of thermodynamic variables (temperature, pressure, density, etc.).

The phase diagram PD_{VAR} of a system interacting through $u_{VAR}(r,X)$ coincides, at any given $\bar{X}$, with the phase diagram PD_{FIX} of the system interacting through the potential $u_{FIX}(r)=\varepsilon f(r/\sigma)$ having identical functional dependence on r, but with fixed energy and size parameters specified by the values $\varepsilon=\varepsilon(\bar{X})$ and $\sigma=\sigma(\bar{X})$. Since the potentials $u_{FIX}(r)$ are conformal, i.e., their plots fall together upon adjusting the values of ε and σ, by *locally* scaling with respect to $\varepsilon(X)$ and $\sigma(X)$ the coordinates of the points laying on PD_{VAR}, the effects of the dependence on X of energy and size parameters are "washed out," and PD_{VAR} is deformed so to match PD_{FIX}. Referring, for example, to variations of temperature, and considering the coexistence curve of a generic phase transition in the T,ρ plane, the following relation holds:

$$\{k_BT/\varepsilon(T),\rho\sigma(T)^3\}_{VAR}=\{k_BT/\varepsilon,\rho\sigma^3\}_{FIX}, \tag{1}$$

where the notation $\{\cdots\}$ indicates the locus of coexisting points.

In spite of the simple ideas involved, the above scaling approach, referred for brevity as state-dependent scaling (SDS), has far-reaching implications. It defines a mapping M from the space S_{VAR} of the phase diagrams of the substances interacting through state-dependent potentials into the space S_{FIX} of the phase diagrams of the substances interacting through state-independent potentials. All phase diagrams corresponding to potentials $u_{VAR}(r,X)$ with identical $f(r)$, and generic functional forms $\varepsilon(X)$ and $\sigma(X)$, are mapped through M into the phase diagram corresponding to the potential $u_{FIX}(r)$ having the same $f(r)$: thus, in spite of apparent diversities, when expressed in state-dependent reduced units, these phase diagrams collapse into a *single* diagram. In virtue of the ensuing equivalence the set of all these elements represents a universality class. This unveils the presence in S_{VAR} of an underlying structure and makes possible to rationalize the wide variety of phase behaviors exhibited by soft matter.

In the light of the above considerations, the usually complex phase diagrams of soft matter can be easily derived from that of simpler substances. As an example, we consider poly-N-isopropylacrylamide (PNIPAM) [8], a thermally re-

sponsive microgel colloid whose interparticle interaction was described [9,10] through the effective temperature-dependent potential

$$u(r,T) = \infty, \quad r < \sigma(T),$$

$$u(r,T) = -\varepsilon(T)[\sigma(T)/r]^8, \quad r \geq \sigma(T). \tag{2}$$

The phase diagram obtained through SDS, using size and energy parameters determined through scattering experiments [10,11], is remarkably close to that calculated through perturbation theory (Fig. 1, top panel). With respect to more sophisticated methods, SDS offers insight due to the ability to enlighten the unexpected relation with familiar behaviors. In the specific case considered, PNIPAM unusual lower-critical-solution-temperature-like point and high-temperature metastable fluid-fluid coexistence are shown to stem (Fig. 1, bottom panel) from the well-known behavior of the reference system, interacting through hard-core repulsion plus inverse power attraction [12].

We now use SDS to investigate inverse melting, i.e., melting upon isobaric cooling, a surprising phenomenon in which the crystal phase has higher molar entropy than the coexisting liquid [13], the reverse of the usual situation. This behavior, envisaged by Tamman about a century ago [14,15] and expected under extreme conditions [16], was recently observed at moderate temperatures and pressures in poly(4-methylpentene-1) (P4MP1) [17] and syndiotactic polystyrene (sPS) [18]. Since the statistical theories presented to explain inverse melting refer to abstract models [19,20], we aim, through the use of SDS, at deriving results more closely related to real polymers. According to recent literature [4,21], effective interactions between the centers of mass of polymers can be represented through the Gaussian pair potential

$$u(r) = \varepsilon e^{-(r/\sigma)2}. \tag{3}$$

This system, called Gaussian core model (GCM), due to the penetrability of the "soft" repulsive core upon increasing density (or pressure), exhibits a melting line with a maximum at a temperature T_S and a reentrant portion [22–24]. The GCM lacks an important feature of real polymeric systems, i.e., the dependence of the size on the temperature. The spatial configuration of a polymer chain results from the balance of repulsive and attractive forces among the elements of the chain. For a given solvent, molecules, swollen at high temperatures due to dominance of excluded volume effects, become progressively more coiled as the temperature decreases, due to the action of attraction, while, at fixed temperature, good and poor solvents cause, respectively, extension or contraction of the chain. From the combination of the above effects, depending on the force field between chain elements, the polymer radius may exhibit a maximum at a temperature T_{max} somewhat greater than the Flory temperature T_θ. Such behavior was observed through experiments [25] and simulation [26]. In particular, simulation results suggest that for good solvents the maximum may be expected to be higher and narrower, while T_{max} becomes closer to T_θ [26] (Fig. 2, inset). To devise a model closer to real polymeric systems we introduce in Eq. (3) a T-dependent σ

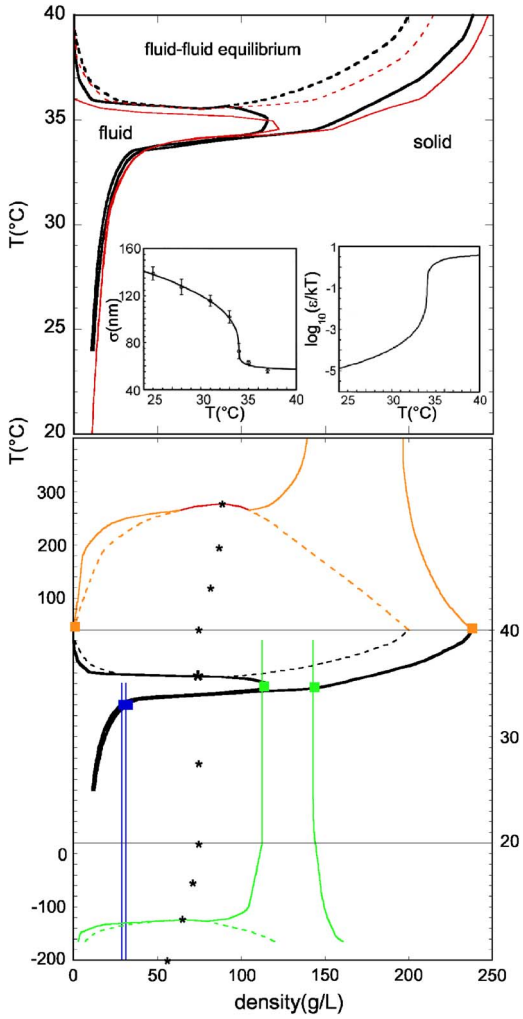

FIG. 1. (Color online) Top panel: PNIPAM phase diagram obtained through SDS (black thick lines: solid, stable coexistence; dashed, metastable coexistence) and through perturbation theory (red thin lines: solid, stable coexistence, dashed, metastable coexistence). Reference potential: $u(r)=\infty$ for $r<\sigma$, $-\varepsilon(\sigma/r)^8$ for $r \geq \sigma$. Size and energy parameters (lower left and lower right inset) as well as perturbation theory result are from Refs. [10,11]. Bottom panel: Phase diagram of the reference system (RS) at $T=33$ °C, 34.5 °C, 40 °C (blue, green, and orange lines, respectively; solid, stable coexistence, dashed, metastable coexistence). In the print version the three phase diagrams can be distinguished from being progressively shifted towards higher densities and temperatures (as T increases from 33 °C to 40 °C). The region 20 °C$\leq T \leq$40 °C is magnified to make PNIPAM phase diagram (black thick lines) visible. Squares represent PNIPAM coexisting points at the three temperatures considered (at $T=33$ °C the two points cannot be resolved on the scale of the figure). Stars represent RS critical point at several temperatures. PNIPAM lower-critical-solution-temperature-like behavior and high-temperature metastable fluid-fluid transition are closely related to RS vapor-liquid coexistence, which is metastable with respect to crystallization (except for a small region around the critical point [12]). PNIPAM metastable region opens up, upon temperature increasing, where the locus of RS critical points intersects PNIPAM freezing line, while, in general, the lower bound of the metastable region lies, for a given density, at the temperature where attraction is no longer strong enough to trigger RS (metastable) condensation.

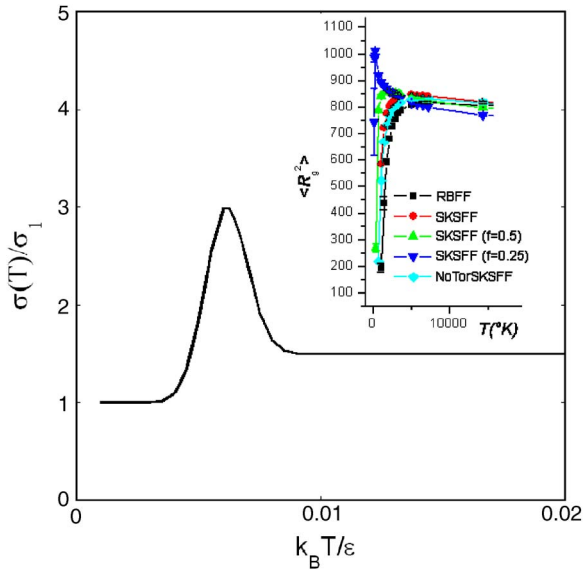

FIG. 2. (Color online) T-dependent size parameter $\sigma(T)$ described in Eq. (4) (parameter values: $T_{\max}=0.7T_S$, $\sigma_1=1$, $\sigma_{\max}=3$, $\sigma_2=1.5$, $\Delta=T_{\max}/5$). Inset: polymeric radius of gyration as a function of temperature for various force fields between the elements of the polymer chain [26]. Solvent effects are included implicitily through a scaling factor f applied to the nonbond potential [28]: smaller values of f correspond to better solvents.

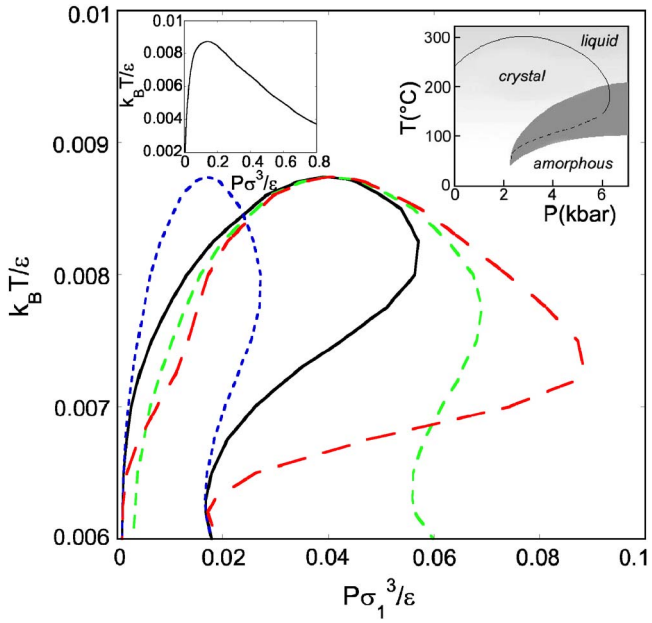

FIG. 3. (Color online) Melting lines, obtained through SDS, of the GCTM. The solid phase is inside the curve. Inverse melting occurs on the portion of the right branch of the curve having positive dT/dP. Parameter values: $T_{max}=0.7T_S$, $\sigma_1=1$; black line: $\sigma_{\max}=3$, $\sigma_2=1.5$, $\Delta=T_{\max}/5$; red line (long dashes): $\sigma_{\max}=3$, $\sigma_2=1.5$, $\Delta=T_{\max}/10$; blue line (short dashes): $\sigma_{\max}=3$, $\sigma_2=2$, $\Delta=T_{\max}/5$; green line (intermediate dashes): $\sigma_{\max}=2$, $\sigma_2=1.5$, $\Delta=T_{\max}/5$. Upper left inset: GCM melting line [24]. Upper right inset: phase diagram of P4MP1, based on structural and calorimetric results [17], with the inverse melting region indicated by the shaded area.

that mimics the behavior of the polymeric radius calculated by simulation [26]. We adopt the simplified form

$$\sigma(T) = \sigma_i + (\sigma_{\max} - \sigma_i)e^{-[(T - T_{\max})//\Delta]^2}, \qquad (4)$$

where $i=1$ for $T \le T_{\max}$ and 2 for $T \ge T_{\max}$, $\sigma_{\max} \ge \sigma_2 \ge \sigma_1$, $T_{\max} > T_\theta$, and Δ is a measure of the maximum width (Fig. 2). Rather than attempting an accurate parametrization of simulation results, the above form aims at catching the main features of polymeric radius dependence on the temperature.

Comparing the melting line of the GCM with T-dependent radius (GCTM) with that of the standard GCM, it appears evident that increasing or decreasing the radius results in shifting the coexisting points (at fixed temperature) towards lower or higher pressures, respectively (Fig. 3). When the radius passes through a maximum, a region of inverse melting may appear on the high pressure branch of the melting line. This region is topologically equivalent to that observed in real systems, the high-pressure, intermediate-temperature GCM fluid corresponding to the high-pressure, intermediate-temperature "amorphous" polymer. The phenomenon is associated with the presence of a temperature interval (for T just larger than T_{max}) where the radius decreases significantly with T, and becomes more evident as the maximum becomes higher or more narrow, and, for fixed maximum height and width, as the value of the radius for $T > T_{\max}$ becomes smaller. Changing T_{max}, the overall behavior remains unaltered, while the concavity on the right portion of the melting line, centered around this temperature, shifts accordingly. To observe any significative deviation from the standard GCM melting line, T_{max} should

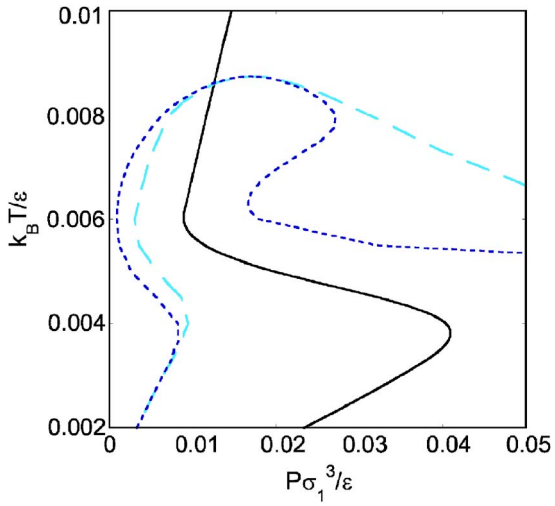

FIG. 4. (Color online) Melting lines, obtained through SDS, for the GCTM and for hard spheres with radius depending on the temperature (HST) as described in Eq. (4). Parameter values: $T_{max}=0.7T_S$, $\sigma_1=1$; blue short-dashed line (GCMT): $\sigma_{\max}=3$, $\sigma_2=2$, $\Delta=T_{\max}/5$; cyan long-dashed line (GCTM) and black solid line (HST): $\sigma_{\max}=\sigma_2=2$, $\Delta=T_{\max}/5$ (in this case the radius increases with T without passing through a maximum). The solid phase is inside the melting line for the GCMT, to its right for HST. Inverse melting at low temperatures occurs on the portion of the melting line with negative dT/dP.

then be smaller than T_S. The results obtained suggest that inverse melting in polymers, at (relatively) high pressures and intermediate temperatures, as is the case for the systems so far investigated [17,18], may be expected when the polymer radius exhibits, at temperatures lower than the freezing temperature, a sufficiently high and narrow maximum. Since measuring polymer size is a simpler task with respect to locating phase boundaries, these results may prove useful to obtain preliminary indications for the occurrence of the phenomenon addressed.

The GCTM considered above exhibits a further region of inverse melting, which occurs on the low pressure branch of the melting line (Fig. 4). The phenomenon is predicted whether or not the radius passes through a maximum, since it is associated with the temperature interval (around T_θ) where the radius increases with T. This condition occurs quite generally, thus inverse melting at low pressures might, in principle, be observed in a greater number of systems. Experimental investigation is called for to explore phase behavior of polymeric systems in this regime. Provided that the radius increases with the temperature, inverse melting is predicted by SDS also for potentials with impenetrable core and melting line without any reentrant portion (Fig. 4). This result appears consistent with the observation of inverse melting characteristics associated with size increase in dense core triblock copolymer micellar systems [27].

In conclusion, state-dependent scaling allows interpretation of phase transitions of systems with variable molecular structure in terms of an intermediate, physically intuitive, level of description, based on the dependence of particle size and interaction strength on thermodynamic parameters. The ensuing analysis is necessarily more coarse grained with respect to microscopical approaches, yet, establishing a bridge over different length scales, is particularly appropriate to describe soft matter, which is characterized by an intrinsically mesoscopic nature.

The author thanks P. V. Giaquinta for helpful discussions.

[1] W. B. Russel, D. A. Saville, and W. R. Schowalter, *Colloidal Dispersions* (Cambridge University Press, Cambridge, England, 1990).
[2] T. A. Witten, *Structured Fluids: Polymers, Colloids, Surfactants* (Oxford University Press, Oxford, England, 2004).
[3] M. Kleman and O. D. Lavrentovich, *Soft Matter Physics: An Introduction* (Springer, New York, 2002).
[4] C. N. Likos, Phys. Rep. **348**, 267 (2001).
[5] J. D. van der Waals, *Verhandelingen Koninklijke Akademie van Wetenschappen* 20 (1880), No. 5, pp. 1–32 and *Verhandelingen Koninklijke Akademie van Wetenschappen* 20 (Amsterdam, 1880) No. 6, pp. 1–11.
[6] J. S. Rowlinson, *J. D. van der Waals, On the Continuity of the Gaseous and the Liquid States*, edited by J. L. Lebowitz, Studies in Statistical Mechanics XIV (North Holland, Amsterdam, 1988).
[7] K. E. Pitzer, J. Chem. Phys. **7**, 583 (1939).
[8] R. H. Pelton and P. Chibante, Colloids Surf. **20**, 247 (1986).
[9] H. Senff and W. Richtering, J. Chem. Phys. **111**, 1705 (1999).
[10] J. Wu, B. Zhou, and Z. Hu, Phys. Rev. Lett. **90**, 048304 (2003).
[11] J. Wu, G. Huang, and Z. Hu, Macromolecules **36**, 440 (2003).
[12] P. J. Camp, Phys. Rev. E **67**, 011503 (2003).
[13] A. Lindsay Greer, Nature (London) **404**, 134 (2000).
[14] G. Tammann, *Kristallisieren und Schmelzen* (Johann Ambrosius Barth, Leipzig, 1903).
[15] G. Tammann and R. F. Mehl, *The States of Aggregation* (Van Nostrand, New York, 1925).
[16] R. Vogel, *Die Heterogenen Gleichgewichte* (Akademische, Leipzig, 1959).
[17] S. Rastogi, G. W. H. Höhne, and A. Keller, Macromolecules **32**, 8897 (1999).
[18] C. S. J. van Hooy-Corstjens, G. W. H. Höhne, and S. Rastogi, Macromolecules **38**, 1814 (2005).
[19] M. R. Feeney, P. G. Debenedetti, and F. H. Stillinger, J. Chem. Phys. **119**, 4582 (2003).
[20] N. Schupper and N. M. Shnerb, Phys. Rev. Lett. **93**, 037202 (2004).
[21] A. A. Louis, P. G. Bolhuis, J. P. Hansen, and E. J. Meijer, Phys. Rev. Lett. **85**, 2522 (2000).
[22] F. H. Stillinger, J. Chem. Phys. **65**, 3968 (1976).
[23] A. Lang, C. N. Likos, M. Watzlawek, and H. Löwen, J. Phys.: Condens. Matter **12**, 5087 (2000).
[24] S. Prestipino, F. Saija, and P. V. Giaquinta, Phys. Rev. E **71**, 050102(R) (2005).
[25] A. Laukkanen, L. Valtola, F. M. Winnik, and H. Tenhu, Macromolecules **37**, 2268 (2004).
[26] Y. Li, Ph.D. thesis, California Institute of Technology, 2004 (unpublished). http://etd.caltech.edu/etd/available/etd-12072004-021118.
[27] K. Mortensen, W. Brown, and B. Nordén, Phys. Rev. Lett. **68**, 2340 (1992).
[28] S. S. Jang, T. Cagin, and W. A. Goddard III, J. Chem. Phys. **119**, 1843 (2003).